

# Electric dipole moment oscillations in Aharonov-Bohm quantum rings

A. M. Alexeev

*School of Physics, University of Exeter, Stocker Road, Exeter EX4 4QL, United Kingdom*

M. E. Portnoi\*

*School of Physics, University of Exeter, Stocker Road, Exeter EX4 4QL, United Kingdom and  
International Institute of Physics, Av. Odilon Gomes de Lima,  
1722, Capim Macio, CEP: 59078-400, Natal - RN, Brazil*

(Dated: 2 August 2011)

Magneto-oscillations of the electric dipole moment are predicted and analyzed for a single-electron nanoscale ring pierced by a magnetic flux (an Aharonov-Bohm ring) and subjected to an electric field in the ring's plane. These oscillations are accompanied by periodic changes in the selection rules for inter-level optical transitions in the ring allowing control of polarization properties of the associated terahertz radiation.

PACS numbers: 73.22.-f, 76.40.+b

## I. INTRODUCTION

Progress in epitaxial techniques has resulted in burgeoning developments in the physics of quantum dots - semiconductor-based 'artificial atoms'. More recently a lot of attention has been turned towards non-simply-connected nanostructures, quantum rings, which have been obtained in various semiconductor systems.<sup>1-3</sup> The fascination in quantum rings is partially caused by a wide variety of purely quantum mechanical effects, which are observed in ring-like nanostructures (for a review see Refs. 4-6). The star amongst them is the Aharonov-Bohm effect,<sup>7,8</sup> in which a charged particle is influenced by a magnetic field away from the particle's trajectory, resulting in magnetic-flux-dependent oscillations of the ring-confined particle energy. The oscillations of the single-particle energy are strongly suppressed by distortion of the ring shape or by applying an in-plane (lateral) electric field, thus reducing the symmetry of the system.<sup>9,10</sup> However, there are other physical quantities, which might have even more pronounced magneto-oscillations when the symmetry of the ring is reduced. For example, in the presence of a lateral electric field exceeding a particular threshold it is possible to switch the ground state of an exciton in an Aharonov-Bohm ring from being optically active (bright) to optically inactive (dark).<sup>11,12</sup> Another hitherto overlooked phenomenon is the flux-periodic change of an electric dipole moment of a quantum ring, which is the main subject of this work.

In Section II we calculate the energy spectrum of an Aharonov-Bohm ring subjected to a lateral electric field. In Section III we consider magneto-oscillations of the ring's electric dipole moment and study their electric field and temperature dependence. The matrix elements of the dipole moment define selection rules for optical transitions. For experimentally attainable quantum rings these transitions occur at terahertz (THz) frequencies. In Section IV we discuss optical selection rules and show how the polarization properties of the associated THz radiation can be tuned by external electric and magnetic fields. Section V contains a brief discussion of the potential applications of the predicted effects.

## II. ENERGY SPECTRUM OF A QUANTUM RING IN A LATERAL ELECTRIC FIELD

The Hamiltonian of an electron confined in an infinitely narrow quantum ring pierced by magnetic flux  $\Phi$  depends only on the polar coordinate  $\varphi$

$$\hat{H}_\Phi = -\frac{\hbar^2}{2M_e R^2} \frac{\partial^2}{\partial \varphi^2} - \frac{i\hbar e}{2\pi} \frac{\Phi}{M_e R^2} \frac{\partial}{\partial \varphi} + \frac{e^2 \Phi^2}{8\pi^2 M_e R^2}, \quad (1)$$

where  $M_e$  is the electron effective mass and  $R$  is the ring radius.

The  $2\pi$ -periodic eigenfunctions of the Hamiltonian defined by Eq. (1) are

$$\psi_m(\varphi) = \frac{e^{im\varphi}}{\sqrt{2\pi}}, \quad (2)$$

and the corresponding eigenvalues are given by

$$\varepsilon_m(f) = \frac{\hbar^2 (m+f)^2}{2M_e R^2} = (m+f)^2 \varepsilon_1(0). \quad (3)$$

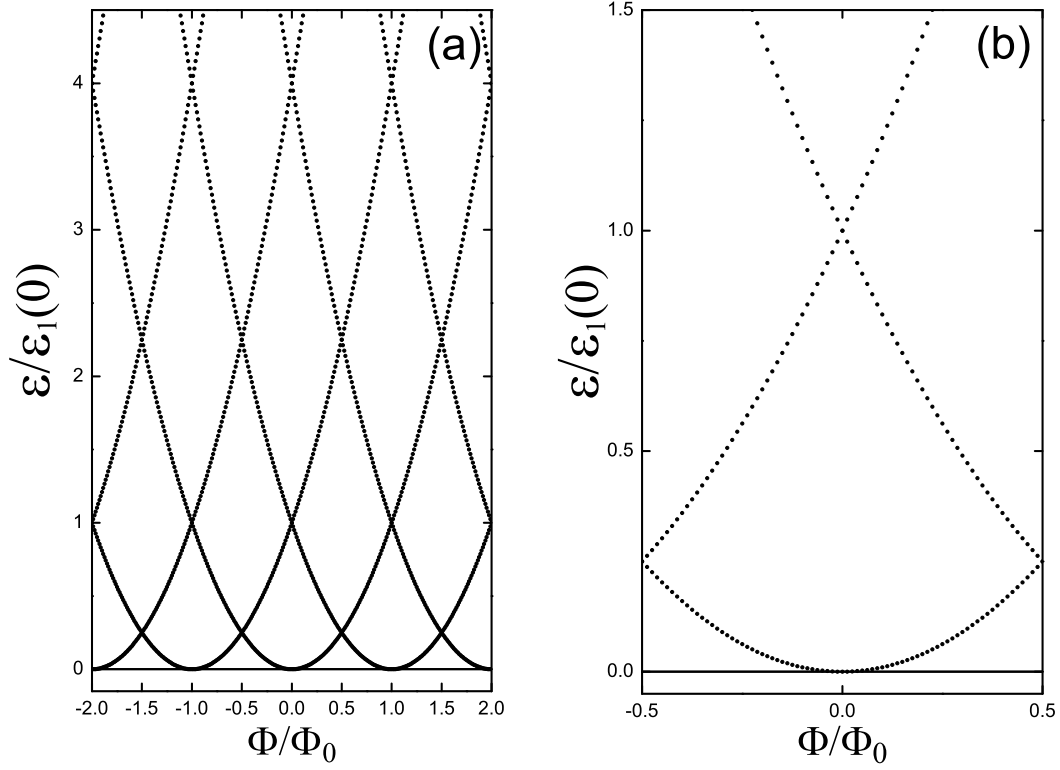


FIG. 1: (a) The energy spectrum of an infinitely narrow quantum ring pierced by magnetic flux  $\Phi$ . Each parabola corresponds to a particular value of the electron angular momentum  $m$ . The electron energies  $\varepsilon$  are plotted versus the number of flux quanta  $\Phi/\Phi_0$ . (b) Expanded view on a smaller energy scale.

Here  $m = 0, \pm 1, \pm 2, \dots$  is the angular momentum quantum number, and  $f = \Phi/\Phi_0$  is the number of flux quanta piercing the ring ( $\Phi_0 = h/e$ ). The electron energy spectrum defined by Eq. (3) is plotted in Fig. 1. It exhibits oscillations in magnetic flux with the period equal to  $\Phi_0$ , known as the Aharonov-Bohm oscillations.<sup>1,8</sup> One can see intersections (degeneracy) of the energy levels with different angular momenta, when  $\Phi$  is equal to an integer number of  $\Phi_0/2$ . Optical selection rules allow transitions between states with angular momentum quantum numbers different by unity ( $\Delta m = \pm 1$ ). For typical nanoscale rings<sup>1,2</sup> the energy scale of the inter-level separation,  $\varepsilon_1(0) = \hbar^2/2M_e R^2$ , is in the THz range. When  $\Phi$  exceeds  $\Phi_0$  the electron possesses a non-zero angular momentum in the ground state.

Applying an in-plane electric field  $\mathbf{E}$  removes the circular symmetry of the system. An additional term corresponding to the electric field appears in the Hamiltonian, which acquires a form

$$\hat{H} = \hat{H}_\Phi + eER \cos \varphi. \quad (4)$$

Now the angle  $\varphi$  is counted from the direction of the electric field. The field mixes electron states with different angular momentum, which is not a good quantum number anymore. An eigenfunction of the Hamiltonian (4), which maintains the  $2\pi$ -periodicity in  $\varphi$ , can be written as a linear combination of the wave functions (2)

$$\Psi_n(\varphi) = \sum_m c_m^n e^{im\varphi}. \quad (5)$$

Substituting the wave function (5) into the Schrödinger equation with Hamiltonian (4), multiplying the resulting expression by  $e^{-im\varphi}$  and integrating with respect to  $\varphi$  leads to an infinite system of linear equations for the coefficients  $c_m^n$

$$\left[ (m+f)^2 - \lambda_n \right] c_m^n + \beta (c_{m+1}^n + c_{m-1}^n) / 2 = 0, \quad (6)$$

where  $\beta = eER/\varepsilon_1(0)$  and  $\lambda_n = \varepsilon_n/\varepsilon_1(0)$ , with  $\varepsilon_n$  being the  $n$ th eigenvalue of the Hamiltonian (4). The energy levels  $\varepsilon_n$  as well as the coefficients  $c_m^n$  can be found numerically by cutting off the sum in Eq. (5) at a particular value of

$|m|$ . The cut-off value should be chosen in compliance with the concerned energy interval, magnitudes of the external fields and required accuracy.

The results of the diagonalization of the matrix corresponding to the system of linear equations (6) are plotted in Fig. 2. In all calculations we chose the cut-off value of  $|m|=11$ . The further increase of the matrix size does not lead to any noticeable change in the results for the considered range of energies and external fields. Interestingly, exactly the same analysis is applicable to a nanohelix subjected to an electric field normal to its axis.<sup>13,14</sup> For a helix the role of magnetic flux is played by the electron momentum along the helical line. In small electric fields the noticeable change in the ring's energy spectrum occurs for the ground state only, in particular, when  $\Phi$  is close to an odd number of  $\Phi_0/2$ . This change in spectrum is associated with the linear in electric field splitting between the ground and first excited states, which were degenerate for  $f = (2m+1)/2$  in the absence of an electric field. First order perturbation theory yields  $\Delta\varepsilon = eER$  as a value of this splitting, which provides a very accurate estimate for the numerical results for  $eER < \hbar^2/2M_eR^2$ . As one can see from Fig. 2, energy oscillations in the ground state are strongly suppressed even for  $eER = 0.2\hbar^2/2M_eR^2$ . This suppression is a major source of difficulty in spectroscopic detection of the Aharonov-Bohm oscillations. However, in the next two sections we show that apart from the ground-state energy there are other physical quantities, such as a dipole moment of the ring and polarization properties of the inter-level transitions, which have highly-pronounced magneto-oscillations when the symmetry of the ring is reduced.

### III. MAGNETO-OSCILLATIONS OF THE ELECTRIC DIPOLE MOMENT

In this section we consider Aharonov-Bohm oscillations of the quantum ring's electric dipole moment. If an electron occupies the  $n$ th state of the neutral single-electron quantum ring with a uniform positive background or a positive charge  $+e$  placed in the ring center, the projection of the dipole moment on the direction of the lateral electric field is given by

$$P_n = eR \int |\Psi_n|^2 \cos \varphi d\varphi. \quad (7)$$

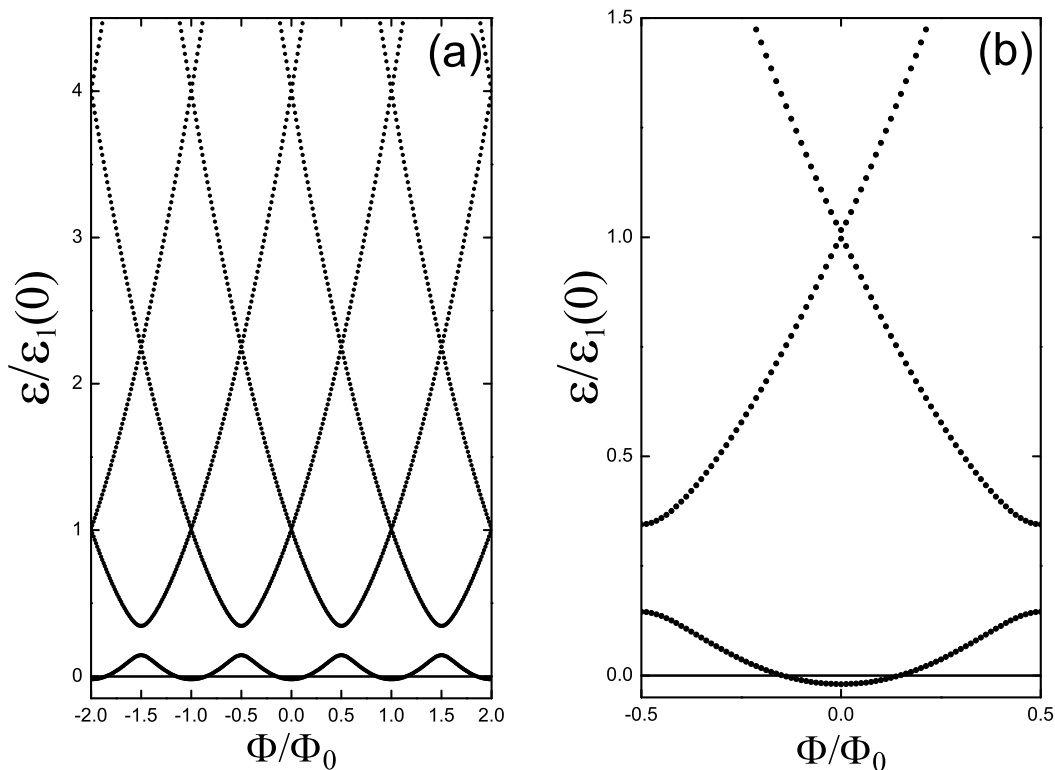


FIG. 2: (a) The energy spectrum of an infinitely narrow quantum ring of radius  $R$  pierced by magnetic flux  $\Phi$  and subjected to an in-plane electric field  $E = 0.2\varepsilon_1(0)/eR$ . The electron energies  $\varepsilon$  are plotted versus the number of flux quanta  $\Phi/\Phi_0$ . (b) Expanded view on a smaller energy scale in which the energy gap  $\Delta\varepsilon = eER$ , opened by the electric field, can be clearly seen.

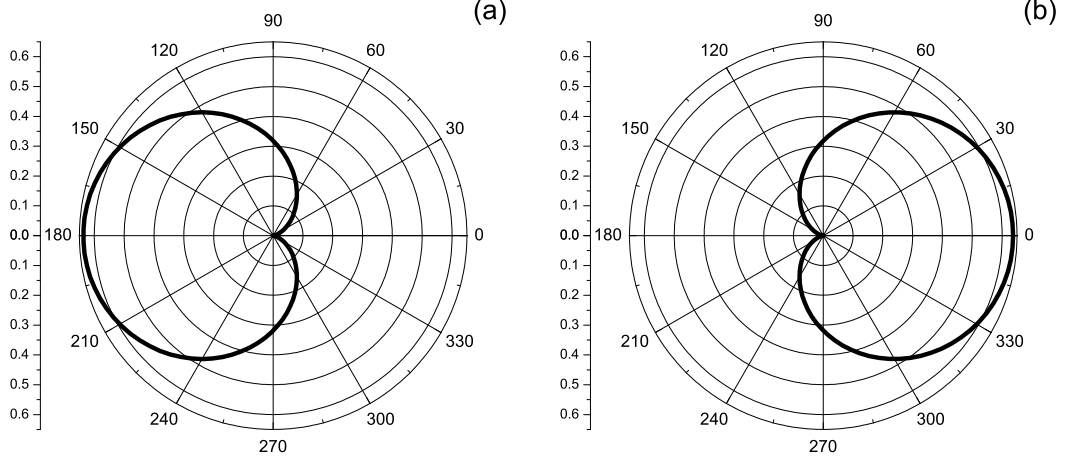


FIG. 3: A polar plot of the electron density distribution in a single-electron quantum ring pierced by a half of the flux quantum and subjected to a weak in-plane electric field,  $E \ll \varepsilon_1(0)/eR$ , applied at the zero angle: (a) for the electron ground state; (b) for the first excited state.

Substituting the wave function (5) into Eq. (7) yields

$$P_n = \frac{eR}{2} \sum_m c_m^n (c_{m-1}^n + c_{m+1}^n), \quad (8)$$

where the coefficients  $c_m^n$  can be found from the system of linear equations (6).

In the absence of an electric field, each of the electron states is characterized by a particular value of angular momentum. Therefore, all the products  $c_m^n c_{m\pm 1}^n$  entering Eq. (8) vanish for any value of  $n$  resulting in the absence of the dipole moment. Let us now consider what happens to the ground state's dipole moment in the presence of a weak electric field,  $eER \ll \hbar^2/2M_e R^2$ . For  $\Phi = 0$ , the ground state is a practically pure  $m = 0$  state with a tiny admixture of  $m \neq 0$  states. However, the situation changes drastically near the point of degeneracy. For  $\Phi = \Phi_0/2$ , even an infinitely small field modifies entirely the wave function of the ground state so that the electron is localized near one side of the ring resulting in the value of the dipole moment being close to  $eR$ . Simultaneously the first excited state has the dipole moment of the same magnitude but the opposite sign. The electron density distributions in the ground and first excited states, when the degeneracy is lifted by a weak electric field, is shown in Fig. 3. With changing magnetic flux the ground state density oscillates with a period  $\Phi_0$  from an unpolarized to a strongly polarized distribution resulting in the corresponding dipole moment oscillations. However, the oscillations of the total dipole moment of the ring should be partially compensated if the first excited state, which carries a dipole moment opposite to the ground state's dipole moment for a flux equal to an odd number of  $\Phi_0$ , is also occupied due to finite temperature. The effect of temperature  $T$  can be taken into account by thermal averaging over all states

$$\langle P \rangle = \frac{\sum_n P_n \exp(-\varepsilon_n/k_B T)}{\sum_n \exp(-\varepsilon_n/k_B T)}. \quad (9)$$

The results of our calculations, using Eq. (9), for several temperature values are shown in Fig. 4. The dipole moment oscillations, which are well-pronounced for  $k_B T \ll eER$ , become suppressed when the temperature increases.

So far we considered the weak electric field limit. For higher fields,  $eER > \hbar^2/2M_e R^2$ , the ground state consists of a mixture of states with different angular momenta for all values of  $\Phi$ . This state is always strongly polarized, with the dipole moment weakly influenced by the flux piercing the ring. The suppression of the dipole moment oscillations with increasing electric field can be seen from Fig. 5, in which the upper curves, corresponding to higher electric fields and higher dipole moments, exhibit less pronounced oscillations.

At this point it would be instructive to discuss conditions needed for an experimental observation of electric dipole moment magneto-oscillations in quantum rings. A typical radius for experimentally attainable rings<sup>1-3</sup> is  $R \simeq 20$  nm. This gives the value of characteristic energy scale of the inter-level separation  $\varepsilon_1(0) \simeq 2$  meV (corresponding to 0.5 THz) for an electron effective mass  $M_e = 0.05m_e$ . For a ring with  $R = 20$  nm, a magnitude of magnetic field producing a flux  $\Phi = \Phi_0$  is  $B \simeq 3$  T. Therefore, the further decrease of the ring radius would require magnetic fields which are hard to achieve. A typical electric field needed for pronounced dipole moment oscillations is  $E = 0.1\varepsilon_1(0)/eR \simeq 10^4$  V/m,

which can be easily created. By far the most difficult condition to be satisfied is the requirement on the temperature regime,  $T < eER/k_B$ . For the discussed electric field and ring radius this condition becomes  $T < 2\text{K}$ . In principle such temperatures can be achieved in laboratory experiments and magneto-oscillations can be detected, for example, in the capacitance measurements. However, for practical device applications, such as quantum-ring-based magnetometry, higher temperatures are desirable. In the next section we consider a process, which is less sensitive to the temperature-induced occupation of excited states.

#### IV. TERAHERTZ TRANSITIONS AND OPTICAL ANISOTROPY

In this section we study the influence of the in-plane electric field on polarization properties of radiative inter-level transitions in Aharonov-Bohm rings. We restrict our consideration to linearly-polarized radiation and dipole optical transitions only. The case of circular polarization is briefly discussed at the end of the section.

The transition rate  $T_{if}$  between the initial ( $i$ ) and final ( $f$ ) electron states is governed by the matrix element  $P_{if} = \langle f | \mathbf{e} \hat{\mathbf{P}} | i \rangle$ , where  $\hat{\mathbf{P}}$  is the dipole moment operator and  $\mathbf{e}$  is the projection of the radiation polarization vector onto the plane of the ring. For our model infinitely-narrow ring

$$P_{if}(\theta) = eR \int \Psi_f^* \Psi_i \cos(\theta - \varphi) d\varphi, \quad (10)$$

where  $\theta$  is the angle between the vector  $\mathbf{e}$  and the in-plane electric field  $\mathbf{E}$ . The geometry of the problem is shown in Fig. 6.

Substituting the electron wave functions  $\Psi_i$  and  $\Psi_f$ , given by Eq. (5), into Eq. (10) yields

$$T_{if} \sim P_{if}^2(\theta) = P_{if}^{-2} + P_{if}^{+2} - 2P_{if}^- P_{if}^+ \cos 2\theta, \quad (11)$$

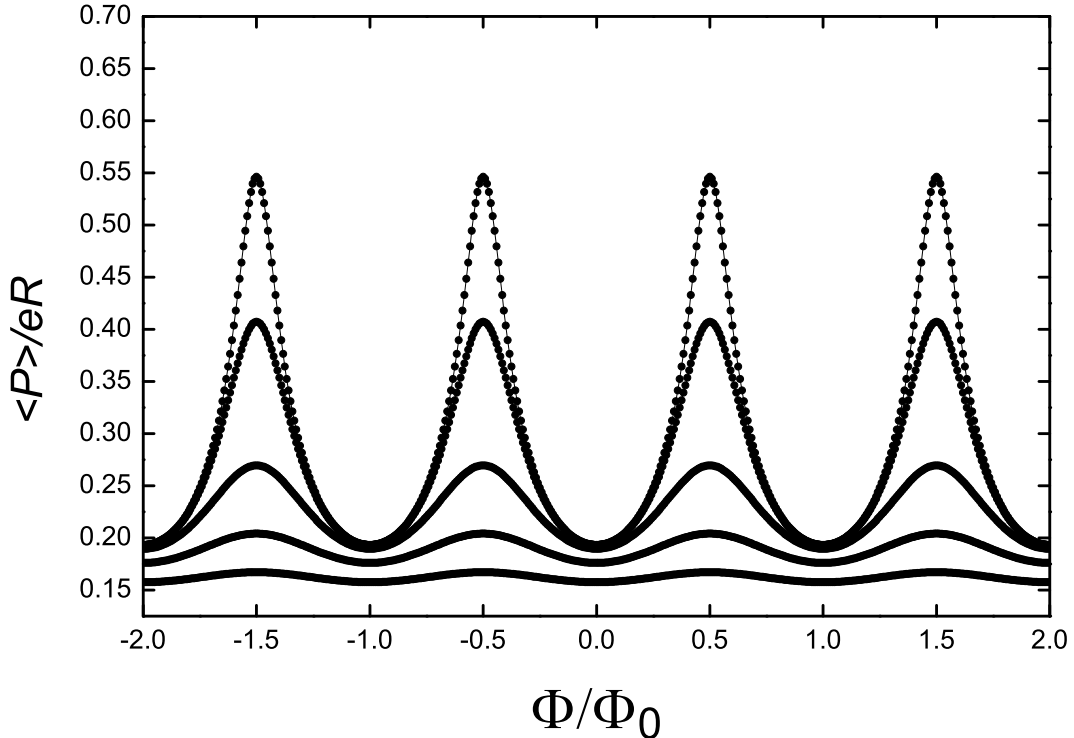


FIG. 4: Magneto-oscillations of the dipole moment of a ring at various temperatures for  $E = 0.2\varepsilon_1(0)/eR$ . Different curves correspond to different temperatures in the range from  $T = 0.01\varepsilon_1(0)/k_B$  to  $T = 0.41\varepsilon_1(0)/k_B$  with the increment  $0.1\varepsilon_1(0)/k_B$ . The upper curve corresponds to  $T = 0.01\varepsilon_1(0)/k_B$ .

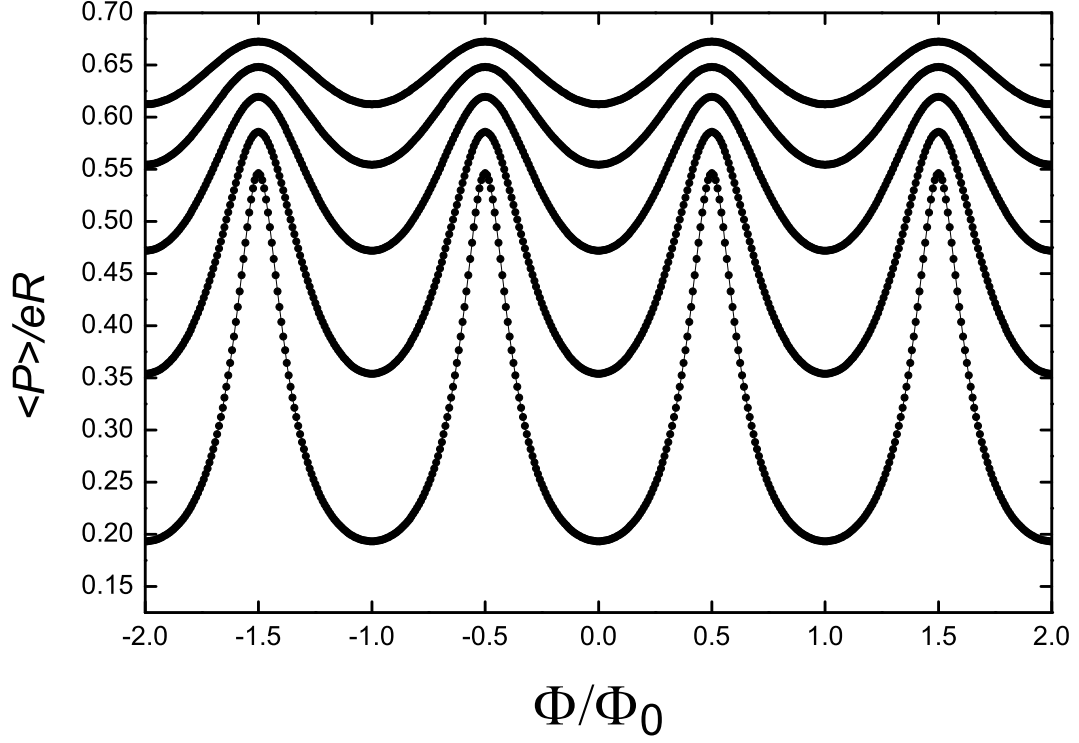


FIG. 5: Magneto-oscillations of the dipole moment of a ring at various magnitudes of the in-plane electric field for  $T = 0.01\varepsilon_1(0)/k_B$ . Different curves correspond to different magnitudes of the electric field in the range from  $E = 0.2\varepsilon_1(0)/eR$  to  $E = 1.0\varepsilon_1(0)/eR$  with the increment  $0.2\varepsilon_1(0)/eR$ . The upper curve corresponds to  $E = 1.0\varepsilon_1(0)/eR$ .

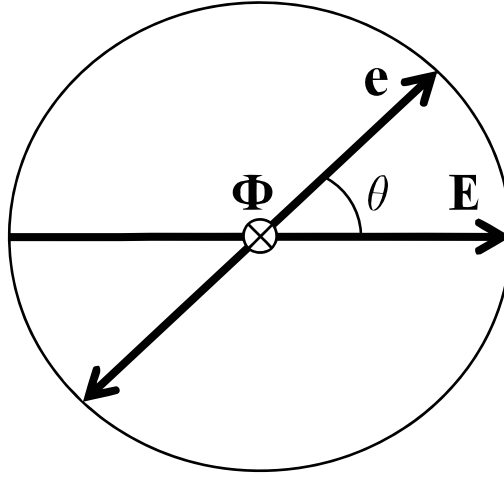


FIG. 6: Relative directions of the external electric field  $\mathbf{E}$  and the projection  $\mathbf{e}$  of the THz radiation polarization vector onto the quantum ring's plane.

where

$$P_{if}^- = \frac{eR}{2} \left| \sum_m c_m^f c_{m-1}^i \right| \quad (12)$$

and

$$P_{if}^+ = \frac{eR}{2} \left| \sum_m c_m^f c_{m+1}^i \right|. \quad (13)$$

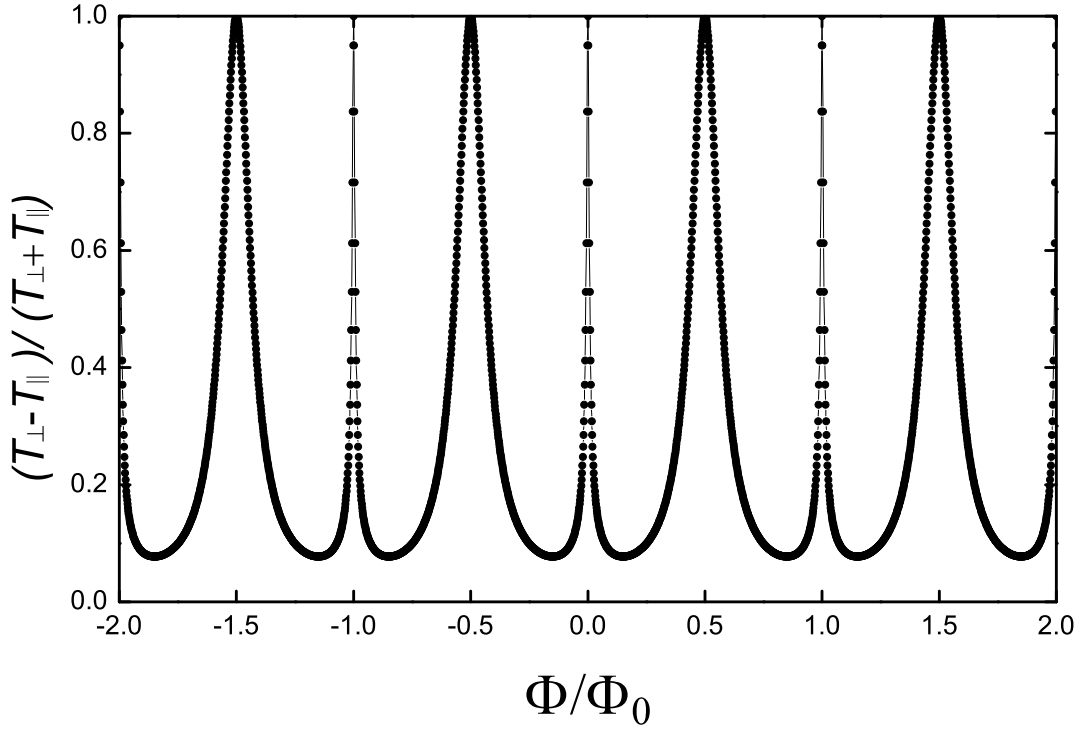


FIG. 7: Magneto-oscillations of the degree of polarization for the transitions between the ground state and the first excited state. Here  $T_{\parallel}$  and  $T_{\perp}$  are correspondingly the intensities of transitions polarized parallel ( $\mathbf{e} \parallel \mathbf{E}$ ) and perpendicular ( $\mathbf{e} \perp \mathbf{E}$ ) to the direction of the in-plane electric field.

The double angle  $2\theta$  entering Eq. (11) ensures that the transition rate does not depend on the sign of  $\mathbf{e}$ .

Let us consider transitions between the ground state and the first excited state of the Aharonov-Bohm ring in a weak in-plane electric field,  $eER \ll \hbar^2/2M_e R^2$ . Away from the points of degeneracy, when these states are characterized with a good accuracy by a definite value of angular momentum, either  $P_{if}^-$  or  $P_{if}^+$  given by Eqs. (12-13) vanishes. As a result, the angular dependence in Eq. (11) disappears and the transitions are completely unpolarized. The picture changes drastically near the points of degeneracy. When  $\Phi$  is equal to an odd integer number of  $\Phi_0/2$  we find  $P_{if}^- = P_{if}^+$ . Therefore, the rate of transitions induced by the radiation polarized parallel to the direction of the in-plane electric field ( $\theta = 0$  or  $\theta = \pi$ ) is equal to zero,  $T_{if} = T_{\parallel} = 0$ . Simultaneously, the rate  $T_{\perp}$  of transitions induced by the light polarized perpendicular to the direction of the in-plane electric field ( $\theta = \pi/2$  or  $\theta = 3\pi/2$ ) reaches its maximum possible value. This leads to a strong optical anisotropy of the system. The results of our calculations for the whole range of  $\Phi$  are shown in Fig. 7. Very sharp peaks at  $\Phi$  equal to an integer number of  $\Phi_0/2$  are the result of splitting between the states, which were degenerate with energy  $\varepsilon_1(0)$  in the absence of an external electric field. This splitting occurs in the second order in  $eER/\varepsilon_1(0)$ . Due to the very small value of the splitting, in comparison with the considered energy scale, the resulting energy gap can not be seen clearly in Fig. 2. These sharp peaks would be smeared if the finite linewidth of the radiation is taken into account.

In the case of circularly polarized light the degree of polarization oscillates as well. Inter-level transitions between the ‘pure’ states, characterized by the definite angular momentum values differing by one, are either right-hand or left-hand polarized. However, one can easily see that transitions involving the states, which are strongly ‘mixed’ when the flux is an integer number of  $\Phi_0/2$ , have the same probabilities for both circular polarizations. Thus, the magnetic-field-induced optical chirality of quantum rings oscillates with the flux.

Total probabilities of the inter-level transitions indeed depend on the populations of the states involved. However, the discussed oscillations of the degree of polarization do not depend on temperature. This effect allows Aharonov-Bohm rings to be used as room-temperature polarization-sensitive detectors of THz radiation or optical magnetometers.

## V. DISCUSSION AND CONCLUSIONS

We have demonstrated that a lateral electric field, which is known to suppress Aharonov-Bohm oscillations in the ground state energy spectrum of a quantum ring, results in strong oscillations of other physical characteristics of the system. Namely, the electric-field-induced dipole moment oscillates as a function of the magnetic flux piercing the ring, with pronounced maxima when the flux is equal to an odd number of one half of the flux quantum. This effect is caused by lifting the degeneracy of states with different angular momentum by arbitrary small electric fields. It should be emphasized that the discussed effect is not an artifact of the infinitely-narrow ring model used in our calculations, but it persists in finite-width rings in a uniform magnetic field. Indeed, the essential feature required for this effect is the degeneracy of the states with the angular momenta differing by one at certain magnetic field values, which is known to take place for finite-width rings as well.<sup>15</sup>

Future observation of the dipole moment magneto-oscillations would require careful tailoring of the ring parameters and experiment conditions. For example, the size of the quantum ring should not exceed the electron mean free path but should be large enough so that, for experimentally attainable magnetic fields, the flux through the ring is near the flux quantum. The electric field should not be too large to avoid polarizing the ring strongly in the absence of a magnetic field, but it should be large enough to achieve a splitting between the ground and first excited states exceeding  $k_B T$ . Our estimates show that all these conditions can be met in existing quantum ring systems. However, the temperature constraint constitutes the major obstacle for any potential applications outside the low-temperature laboratory.

The temperature restrictions are less essential for another predicted effect - giant magneto-oscillations of the polarization degree of radiation associated with inter-level transitions in Aharonov-Bohm rings. Notably, these transitions for the rings satisfying the remaining constraints should occur at THz frequencies. Creating reliable, portable and tuneable sources of THz radiation is one of the most formidable problems of contemporary applied physics. The unique position of the THz range in between the frequencies covered by existing electronic or optical mass-produced devices results in an unprecedented variety of ideas aiming to bridge the so-called ‘THz gap’. For example, the proposed methods of down-conversion of optical excitation range from creating ultra-fast saturable absorbers<sup>16</sup> to utilizing magnetic-field-induced energy gap in metallic carbon nanotubes<sup>17–19</sup> to recent proposals of exciting THz transitions between exciton-polariton branches in semiconductor microcavities.<sup>20,21</sup> Arguably, the use of quantum rings for THz generation and detection has its merits, since their electronic properties can be easily tuned by external fields. The following scheme for using Aharonov-Bohm quantum rings as tuneable THz emitters can be proposed. Inversion of population in semiconductor quantum rings or type II quantum dots can be created by optical excitation across the semiconductor gap. Angular momentum and spin conservation rules do not forbid the creation of an electron in the first excited state as long as the total selection rules for the whole system, consisting of an electron-hole pair and a photon causing this transition, are satisfied. Terahertz radiation will be emitted when the electron undergoes a transition from the excited to the ground state of the ring. As was shown in the previous sections both the frequency and polarization properties of this transition can be controlled by external magnetic and electric fields.

Other potential applications of the discussed effects are in the burgeoning areas of quantum computing and cryptography. The discussed mixing of the two states, which are degenerate in the absence of electric field, is completely controlled by the angle between the in-plane field and a fixed axis. This brings the potential possibility for creating nanoring-based qubits, which do not require weak spin-orbit coupling between the electric field and electron spin. Arrays of the Aharonov-Bohm rings can also be used for polarization sensitive single-photon detection, which is essential for quantum cryptography.

## Acknowledgments

This work was supported by the FP7 Initial Training Network Spin-Optronics (Grant No. FP7-237252) and FP7 IRSES projects SPINMET (Grant No. FP7-246784), TerACaN (Grant No. FP7-230778), and ROBOCON (Grant No. FP7-230832). We are grateful to A. V. Shytov for fruitful discussions and to C. A. Downing for a critical reading of the manuscript and for helpful suggestions.

---

\* Corresponding author: M.E.Portnoi@exeter.ac.uk

<sup>1</sup> A. Lorke, R. J. Luyken, A. O. Govorov, J. P. Kotthaus, J. M. Garcia, and P. M. Petroff, Phys. Rev. Lett. **84**, 2223 (2000).

<sup>2</sup> E. Ribeiro, A. O. Govorov, W. Carvalho, Jr., and G. Medeiros-Ribeiro, Phys. Rev. Lett. **92**, 126402 (2004).



- <sup>3</sup> J. X. Chen, W. S. Liao, X. Chen, T. L. Yang, S. E. Wark, D. H. Son, J. D. Batteas, and P. S. Cremer, ACS Nano **3**, 173 (2009).
- <sup>4</sup> A. G. Aronov and Yu. V. Sharvin, Rev. Mod. Phys. **59**, 755 (2004).
- <sup>5</sup> S. Viefers, P. Koskinen, P. Singha Deo, and M. Manninen, Physica E (Amsterdam) **21**, 1 (2004).
- <sup>6</sup> T. Ihn, A. Fuhrer, L. Meier, M. Sigrist, and K. Ensslin, Europhysics News **36**, 78 (2005).
- <sup>7</sup> W. Ehrenberg and R. E. Siday, Proc. Phys. Soc. London Sect. B **62**, 8 (1949).
- <sup>8</sup> Y. Aharonov and D. Bohm, Phys. Rev. **115**, 485 (1959).
- <sup>9</sup> Z. Barticevic, G. Fuster, and M. Pacheco, Phys. Rev. B **65**, 193307 (2002).
- <sup>10</sup> A. Bruno-Alfonso and A. Latgé, Phys. Rev. B, **71**, 125312 (2005).
- <sup>11</sup> A. M. Fischer, V. L. Campo, Jr., M. E. Portnoi, and R. A. Römer, Phys. Rev. Lett. **102**, 096405 (2009).
- <sup>12</sup> M. D. Teodoro, V. L. Campo, Jr., V. Lopez-Richard, E. Marega, Jr., G. E. Marques, Y. Galvão Gobato, F. Iikawa, M. J. S. P. Brasil, Z. Y. AbuWaar, V. G. Dorogan, Yu. I. Mazur, M. Benamara, and G. J. Salamo Phys. Rev. Lett. **104**, 086401 (2010).
- <sup>13</sup> O. V. Kibis, S. V. Malevannyy, L. Huggett, D. G. W. Parfitt, M. E. Portnoi, Electromagnetics **25**, 425 (2005).
- <sup>14</sup> O. V. Kibis and M. E. Portnoi, Tech. Phys. Lett. **33**, 878 (2007).
- <sup>15</sup> M. E. Portnoi, O. V. Kibis, V. L. Campo Jr, M. Rosenau da Costa, L. Huggett, and S. V. Malevannyy, Proc. 28th ICPS, AIP Conference Proceedings **893**, 703 (2007).
- <sup>16</sup> E. A. Avrutin and M. E. Portnoi, Sov. Phys. Semicond. **22**, 968 (1988).
- <sup>17</sup> M. E. Portnoi, O. V. Kibis, M. Rosenau da Costa, Superlatt. Microstruct. **43**, 399 (2008).
- <sup>18</sup> M. E. Portnoi, M. Rosenau da Costa, O. V. Kibis, and I. A. Shelykh, Int. J. Mod. Phys. B **23**, 2846 (2009).
- <sup>19</sup> K. G. Batrakov, O. V. Kibis, P. P. Kuzhir, M. Rosenau da Costa, and M. E. Portnoi, J. Nanophoton. **4**, 041665 (2010).
- <sup>20</sup> K. V. Kavokin, M. A. Kaliteevski, R. A. Abram, A. V. Kavokin, S. Sharkova, and I. A. Shelykh, Appl. Phys. Lett. **97**, 201111 (2010).
- <sup>21</sup> E. del Valle and A. Kavokin, Phys. Rev. B **83**, 193303 (2011).